

DOI: 10.1002/cssc.201200419

Ketonic Decarboxylation Reaction Mechanism: A Combined Experimental and DFT Study

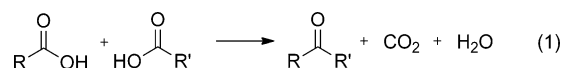
Angeles Pulido,* Borja Oliver-Tomas, Michael Renz,* Mercedes Boronat, and Avelino Corma^[a]

The ketonic decarboxylation of carboxylic acids has been carried out experimentally and studied theoretically by DFT calculations. In the experiments, monoclinic zirconia was identified as a good catalyst, giving high activity and high selectivity when compared with other potential catalysts, such as silica, alumina, or ceria. It was also shown that it could be used for a wide range of substrates, namely, for carboxylic acids with two to eighteen carbon atoms. The reaction mechanism for the ketonic decarboxylation of acetic acid over monoclinic zir-

conia was investigated by using a periodic DFT slab model. A reaction pathway with the formation of a β -keto acid intermediate was considered, as well as a concerted mechanism, involving simultaneous carbon-carbon bond formation and carbon dioxide elimination. DFT results showed that the mechanism with the β -keto acid was the kinetically favored one and this was further supported by an experiment employing a mixture of isomeric (linear and branched) pentanoic acids.

Introduction

The conversion of biomass, instead of fossil fuels, into chemicals and fuels is one of the most relevant research areas at the present time and is important for both academia and industry.^[1–3] Biomass consists of highly oxy-functionalized molecules and, for fuels and chemicals production, the carbon/oxygen ratio needs to be increased. Thus, to upgrade biomass molecules, they have to be initially dehydrated and hydrogenated, whereas the molecular size has to be increased, by means of C–C bond formation reaction, especially for the production of liquid transportation fuels, and oxy functionalities have to be removed. One of the routes that allows controlled C–C coupling and deoxygenation is decarboxylation of carboxylic acids, also known as ketonic decarboxylation, in which two carboxylic acids, abundant in the biomass, are transformed into a ketone with water and carbon dioxide as the only byproducts. The ketonic decarboxylation reaction can be written as shown in Equation (1):



If only one acid is used as a reactant in Equation (1) ($\text{R}=\text{R}'$), then the product is a symmetric ketone ($\text{R}-\text{CO}-\text{R}$), whereas if

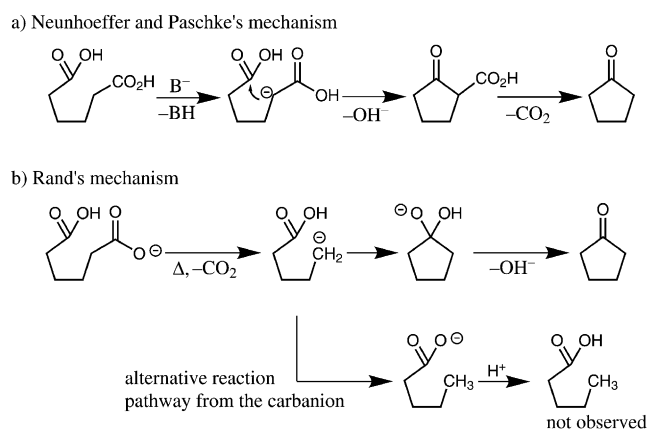
the reaction takes place between two different carboxylic acids ($\text{R}\neq\text{R}'$), then a mixture of three ketones is obtained: two symmetrical ($\text{R}-\text{CO}-\text{R}$ and $\text{R}'-\text{CO}-\text{R}'$) and one asymmetrical ($\text{R}-\text{CO}-\text{R}'$). Furthermore, note that fatty ketones, from decarboxylation of fatty acids, are valuable items in the chemical industry and find applications in ink manufacturing,^[4] detergents,^[5] or in personal care products.^[6] Many examples for ketonic decarboxylation starting from one carboxylic acid can be found in industry. Dry distillation of calcium acetate to yield acetone was reported in 1858 and has been used for the commercial manufacture of acetone over 50 years.^[7] However, acetone formation is only one of the possible examples and production of symmetrical and asymmetrical ketones (such as 2-pentanone,^[8] 3-pentanone,^[9] cyclopentanone^[10,11] or propiophenone,^[8,12] among others^[13–16]) reported. More recently, ketonic decarboxylation has been proposed by Dumesic et al. as a key step for the upgrading of valeric acid, which can be obtained, for instance, from cellulose, to produce liquid transportation fuels.^[17] The primary product, namely 5-nonanone, can be hydrogenated to nonane and included in the kerosene fraction.

It has been observed that ketonic decarboxylation takes place over a wide range of metal oxide catalysts (such as MgO, BaO, CeO₂, ZrO₂, or TiO₂, and mixtures thereof among others),^[13,15,18–36] although a preferred catalyst cannot be identified. Therefore, it is of paramount interest for the further development of biomass transformations to optimize the catalytic process for the conversion of acids into ketones and to select the most suitable metal oxide catalyst. To control the catalytic process, it is crucial to have a good understanding of the reaction mechanism of ketonic decarboxylation and it is desirable to have a deep insight into the most favorable reaction pathways of the mechanism, as well as possible competitive routes. To date, controversy exists about the reaction mechanism that

[a] Dr. A. Pulido, B. Oliver-Tomas, Dr. M. Renz, Dr. M. Boronat, Prof. A. Corma
Instituto de Tecnología Química, Universitat Politècnica de València
Consejo Superior de Investigaciones Científicas (UPV-CSIC)
Av. de los Naranjos s/n, 46022 Valencia (Spain)
Fax: (+34) 96 387 9444
E-mail: apulido@itq.upv.es
mrenz@itq.upv.es

Supporting Information for this article is available on the WWW under
<http://dx.doi.org/10.1002/cssc.201200419>.

takes place during ketonic decarboxylation. In 1939, Neunhoeffer and Paschke proposed a reaction mechanism for cyclopentanone formation from adipic acid by means of a β -keto acid intermediate, formed by abstraction of an α -hydrogen atom, H_α (Scheme 1).^[10] This mechanism has been further dis-



Scheme 1. Reaction mechanism for ketonic decarboxylation involving a) a β -keto acid, proposed by Neunhoeffer and Paschke,^[10] and b) the mechanism proposed by Rand et al.^[13]

ussed by other authors with different substrates and reaction conditions, involving fixed-bed, continuous-flow reactors.^[21,37] Miller et al. reported ketonic decarboxylation of isobutyric acid, lacking hydrogen atoms in the alpha position, over an aerogel thoria catalyst for the formation of the asymmetric *tert*-butyl isobutyl ketone with no evidence of di-*tert*-butyl ketone.^[24] They proposed that acids without alpha-hydrogen atoms may be ketonically decarboxylated through a reaction occurring at the beta carbon and resulting in an asymmetrical ketone. Another argument in favor of this mechanism reported by Koch and Leibnitz was the impossibility of obtaining a ketone product from 2,2,5,5-tetramethyladipic acid or pivalic acid,^[37] molecules without any H_α atom. However, in 1962, the formation of 2,2,5,5-tetramethylcyclopentanone from 2,2,5,5-tetramethyladipic acid was reported by Rand et al., and this cyclization reaction could not be explained by the β -keto acid mechanism previously proposed.^[13] They suggested that the reaction substrate was the mono-deprotonated diacid (Scheme 1).^[13] Thus, the deprotonated acid functionality is decarboxylated, forming a carbanion that preferentially attacks the remaining carboxylic acid group nucleophilically. However, an inconsistency was pointed out for this proposed mechanism:^[15] the carbanion formed should be protonated to a large extent by the carboxylic acid to form pentanoic acid (described as an alternative reaction pathway in Scheme 1), but this product has never been reported. A further development of Rand's mechanism has been proposed by one of us,^[15] in which the decarboxylation and nucleophilic attack occur in a concerted fashion, avoiding significant drawbacks of Rand's mechanism. It is also necessary to take into account that, if the decarboxylation reaction involves temperatures above 450 °C, pyrolysis of the carboxylic acid will be a competitive route leading to the formation of a series of undesired byproducts. Pyrolysis of calcium decanoate was investi-

gated by Hites and Biemann, and they proposed a free-radical mechanism in which alkyl and acyl radicals acted as initiators.^[38]

Valuable knowledge about the reaction mechanism of ketonic decarboxylation can be extracted from the proposed pathways taking place during adipic acid decarboxylation.^[10,13] However, this is a particular case and the transfer of this knowledge to the ketonic decarboxylation of fatty acids in the biomass is not so straightforward for the following reasons: 1) cyclopentanone can be obtained in excellent yield at much lower reaction temperatures (250–300 °C) than those required for monocarboxylic acids (350 to 400 °C); and 2) it is an intramolecular reaction, whereas we will be dealing mainly with intermolecular reactions during biomass transformations. Therefore, we focused on the intermolecular ketonic decarboxylation of monocarboxylic acids catalyzed by metal oxides. The use of computational chemistry is highly desired to provide mechanistic insight on the molecular scale, since no direct experimental evidence about transition-state structures and other mechanistic details can be obtained. Although some computational studies on ketonic decarboxylation over metal oxides are available in the literature, they mainly focus on water and acid adsorption,^[39–41] and a detailed mechanistic investigation is still missing. Herein, we report the excellent performance of monoclinic zirconia oxide as a catalyst for ketonic decarboxylation with very high reaction yields and selectivity towards the ketone, regardless of whether light or fatty acids, such as acetic or stearic acid, were used as reactants. Moreover, the reaction mechanism of acetone formation over monoclinic zirconia (*m*-ZrO₂) was investigated by means of a periodic DFT model. The two previously proposed reaction mechanisms, described above,^[10,13] as well as competitive reaction routes^[38] were investigated, and a general overview of the ketonic decarboxylation reaction mechanism is given.

Experimental Section

General

Acetic acid, pentanoic acid, decanoic acid, and stearic acid were purchased from standard chemical suppliers, such as Acros or Aldrich, and used as received. Monoclinic zirconium oxide and silicon oxide were bought from ChemPur, Germany, as pellets with surface areas of 100 and 240 m²g⁻¹, respectively. CeO₂ (nanopowder, 64 m²g⁻¹) and Al₂O₃ (pellets, 330 m²g⁻¹) were obtained from Aldrich. ZrCeO₄ (70 m²g⁻¹) was synthesized by following a literature procedure.^[42]

Ketonic decarboxylation in a fixed-bed, continuous-flow reactor

The reaction apparatus is displayed in Figure 1. The catalyst (2.5 g, pellets 0.4–0.8 mm) was diluted with silicon carbide and placed as a fixed bed in a stainless-steel tube (0.93 cm external diameter). The reactor was heated to reaction temperature T_r and the feed (5 mL) was passed through at a rate of 9.0 mLh⁻¹ together with a nitrogen flow of 50 mLmin⁻¹ at ambient pressure. The product was condensed at room temperature and analyzed offline by gas chromatography with dodecane as an external standard.

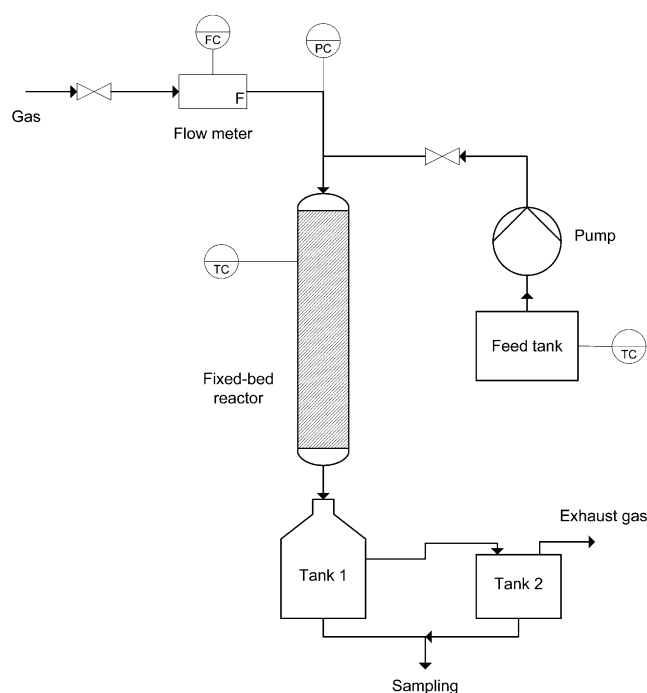


Figure 1. Schematic description of the fixed-bed, continuous-flow reactor employed for gas-phase ketonic decarboxylation. FC = flow controller, PC = manometer, TC = temperature controller.

Computational Methods

The stable phase of zirconium dioxide at low pressure between 0 and 1180 °C has monoclinic symmetry (space group $P2_1/c$) and its experimental structure (lattice parameters $a = 5.150$ Å, $b = 5.212$ Å, $c = 5.315$ Å, and $\beta = 99.23^\circ$) was taken as the initial setup for modeling bulk m -ZrO₂. The DFT-optimized lattice vectors of m -ZrO₂ were obtained from a Birch–Murnaghan fit^[43,44] and were found to be 1.2% larger than the experimental value ($a = 5.21$ Å, $b = 5.27$ Å, and $c = 5.38$ Å). Periodic DFT calculations were carried out with the VASP code^[45] using the PW91 functional,^[46,47] and core electrons were described by using a projector-augmented-wave method (PAW), as described by Blöchl^[48] and adopted by Kresse and Joubert.^[49] For the Zr atoms, a total of 12 electrons ($4s^2 4p^6 5s^2 4d^2$) were treated explicitly. DFT volume calculations were performed by using a $4 \times 4 \times 4$ k-point set, which corresponds to 16 irreducible k-points, and a plane wave basis set with an energy cutoff of 800 eV.

The relative stability of the seven inequivalent surfaces of m -ZrO₂ has previously been investigated at the periodic DFT level by Christensen and Carter,^[50] and the $(\bar{1}11)$ surface has been found to be the most stable one. Therefore, the m -ZrO₂ surface was modeled by using a periodic $(\bar{1}11)$ facet slab model built up as follows: from the DFT-optimized bulk m -ZrO₂, the $(\bar{1}11)$ facet surface was built up with surface vectors along the $[110]$ and $[101]$ directions with lengths of 6.86 and 7.41 Å, respectively (see Figure 2) and a distance of about 20 Å between periodic images. This unit cell contained three ZrO₂ layers and had a chemical composition of Zr₁₂O₂₄. The mechanistic investigation was carried out by using a periodic $(\bar{1}11)$ facet slab model, denoted m -ZrO₂($\bar{1}11$), with a $2 \times 2 \times 1$ supercell and a composition of Zr₄₈O₉₆; see the Supporting Information for additional details.

Geometry optimization was performed at the periodic PW91 level by fixing the coordinates of the Zr and O atoms in the lowermost ZrO₂ layer, whereas all other atoms were fully relaxed until forces

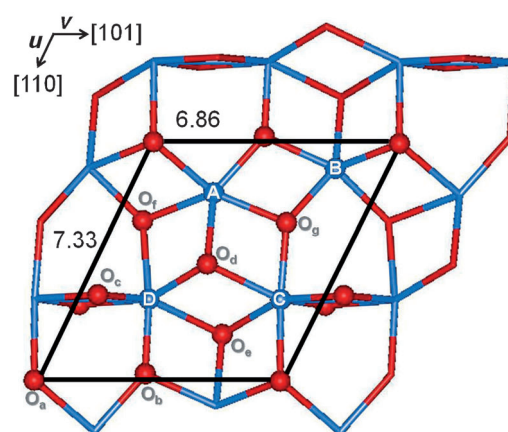


Figure 2. PW91-optimized unit cell of the $(\bar{1}11)$ facet surface of the m -ZrO₂ model. Inequivalent zirconium (Zr_{A–D}) and oxygen (O_{a–g}) atoms are indicated. Distances of the surface vectors (u and v) are given in Å. Zr and O atoms are depicted in light and dark gray, respectively.

were below $0.015 \text{ eV \AA}^{-1}$ using only one irreducible k point and a plane wave basis set with an energy cut off of 500 eV. Optimization of the transition-state structure was performed with the dimer method by using only first derivatives^[51] and the nudged elastic band method, as implemented by Henkelman and Jónsson.^[52] Electronic PW91 energies were further corrected by the addition of intermolecular dispersion energies, which were evaluated by using the D3 method,^[53,54] over the PW91-optimized geometries.

Results and Discussion

With the aim of understanding the ketonic decarboxylation reaction at the molecular scale, a combined theoretical and experimental study has been carried out. First, the performance of several metal oxide catalysts, such as alumina, silica, ceria, zirconia, and mixed zirconium cerium oxide, in the decarboxylation of decanoic acid into 10-nonadecanone has been investigated experimentally when placed as fixed beds in a continuous-flow reactor. From this series of experiments employing different catalysts, and based on characteristics such as selectivity towards ketone, reaction temperature, and conversion, zirconia was selected as the best catalyst and submitted to further investigations. Thus, the catalytic performance of zirconium dioxide for ketonic decarboxylation of a series of carboxylic acids, containing from two to eighteen carbon atoms, was studied. Then, quantum chemistry was used to investigate, in detail, the reaction pathways taking place during ketonic decarboxylation of acetic acid over zirconium dioxide by using a periodic DFT-D model. Finally, the ketonic decarboxylation reaction mechanism is discussed.

Experimental study on ketonic decarboxylation over different metal oxides

The ketonic decarboxylation of decanoic acid was carried out at 350, 375, 400, and 425 °C over zirconia, ceria, mixed zirconium cerium oxide, silica, and alumina. The conversion and selectivity for these reactions are displayed in Figure 3. Conver-

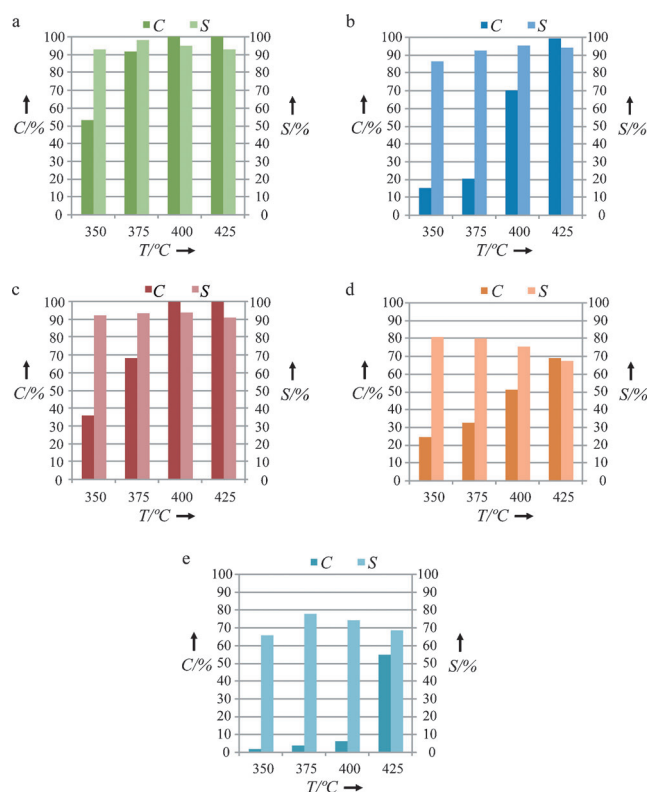


Figure 3. Conversion (C) and selectivity (S) for the ketonic decarboxylation of decanoic acid, contact time weight of catalyst/feed rate (W/F) = 0.31 g h g⁻¹, over different metal oxides: a) ZrO₂, b) CeO₂, c) CeZrO₄, d) SiO₂, and e) Al₂O₃.

sion increased when raising the temperature and full conversion was observed at 400 °C with zirconium oxide and zirconium cerium mixed oxide, and at 425 °C with cerium oxide (Figure 3a, c, and b, respectively). The mixed oxide CeZrO₂ behaves exactly the same as a mixture of the pure oxides CeO₂ and ZrO₂ when the decline in conversion is considered below 400 °C (cf. Figure 3c). For these three cases the selectivity reached 90 to 95% in almost all cases. The other two oxides employed, that is, SiO₂ and Al₂O₃, were significantly less active. With silica, conversion increased successively with temperature up to 70% at 425 °C, but the selectivity was never higher than 80% and varied between 65 and 80% (Figure 3d). Al₂O₃ gave low conversions over almost the whole temperature range (Figure 3e).

The most favorable reaction conditions identified, with decanoic acid as the substrate, were achieved with the use of commercial pelletized *m*-ZrO₂ at 400 °C for which full conversion was obtained together with 95% selectivity towards the desired ketone. However, almost the same results were achieved with the zirconium cerium mixed oxide at the same temperature or with cerium oxide at 425 °C. Because the cerium oxide and zirconium cerium mixed oxide had significantly lower activity at temperatures below 400 °C in comparison to zirconium oxide, the latter was chosen for screening carboxylic acids with different carbon chain lengths and a total carbon atom number from two to eighteen. Similar trends were observed for all carboxylic acids when passed at the same feed

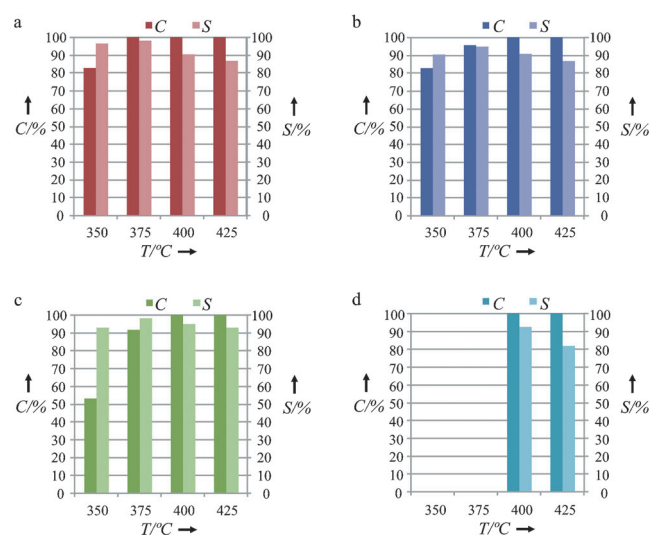
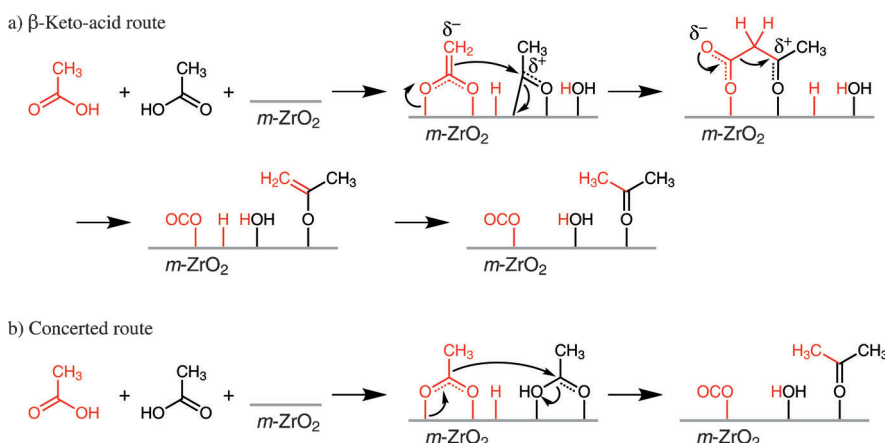


Figure 4. Conversion and selectivity for the ketonic decarboxylation of different carboxylic acids over ZrO₂ (2.5 g) when employing a feed rate of 9 mL min⁻¹: a) acetic acid (C₂H₄O₂; contact time W/F = 0.26 g h g⁻¹; 15.9 g h mol⁻¹), b) valeric (pentanoic) acid (C₅H₁₀O₂; contact time W/F = 0.30 g h g⁻¹; 30.5 g h mol⁻¹), c) decanoic acid (C₁₀H₂₀O₂; contact time W/F = 0.31 g h g⁻¹; 53.5 g h mol⁻¹), and d) stearic acid (C₁₈H₃₆O₂; contact time W/F = 0.33 g h g⁻¹; 81.4 g h mol⁻¹).

rate (9.0 mL h⁻¹, see Figure 4). Hence, conversion was complete in all cases at a reaction temperature of 400 °C, for acetic acid even at 375 °C (see Figure 4a). The selectivity varied between 90 and 95%, with the exception of a reaction temperature of 425 °C, where in many cases the selectivity dropped below 90%. Very similar results were obtained when the reaction was compared at the same contact time for the weight of catalyst and time per mol of substrate for the four carboxylic acids (for details see the Supporting Information).

From these experimental results, it can be concluded that monoclinic zirconium oxide is a suitable catalyst for the ketonic decarboxylation of carboxylic acids with a wide range of molecular weights, that is, from acetic acid to fatty acids.

Thus, to understand the ketonic decarboxylation reaction mechanism at the molecular scale, the formation of acetone (CH₃-CO-CH₃), carbon dioxide (CO₂), and water (H₂O) from the decarboxylation of two molecules of acetic acid (CH₃-COOH) was investigated by using DFT. Taking into account the experimental results presented before, we have chosen *m*-ZrO₂, modeled as a (111) facet surface by using a periodic slab model, *m*-ZrO₂(111), as catalysts for the DFT study. Based on the previously proposed reaction mechanisms^[10,13] described above for adipic acid (see Scheme 1), decarboxylation of acetic acid was investigated via formation of a β-keto acid intermediate and through a concerted route, based on a modification of Rand's mechanism (see Scheme 2). Thus, intermediate and transition-state structures along the reaction pathways following a β-keto acid or a concerted route were identified, as well as other competitive routes.



Scheme 2. Reaction mechanism for acetic acid decarboxylation over m -ZrO₂ via the β -keto acid (a) and concerted (b) routes.

DFT investigation of acetic acid decarboxylation over m -ZrO₂

In the case of gas-phase reactions on solid catalysts, adsorption of reactant molecules over the catalyst surface is the first step of the reaction mechanism. In the case of metal oxide catalysts, factors such as surface topology or surface metal and oxygen atom coordination can play a crucial role in the reaction mechanism.^[55] Thus, the reactivity of zirconium and oxygen atoms of the $(\bar{1}11)$ facet surface of m -ZrO₂ are discussed first. The unit cell of the periodic m -ZrO₂ ($\bar{1}11$) surface slab model has four zirconium atoms (Zr_{A-D}) and seven oxygen atoms (O_{a-g}) per layer, which are not equivalent (see Figure 2). Three out of the four zirconium atoms (Zr_A, Zr_B, and Zr_C) are sixfold coordinated, denoted herein as 6-fc, whereas the last zirconium, Zr_D, is 7-fc. Zirconium atoms in bulk m -ZrO₂ are 7-fc, whereas oxygen atoms are 3- or 4-fc. Therefore, the Zr_D atom is expected to be inert towards acetic acid molecule adsorption due to the lack of coordination vacancies, whereas the 6-fc zirconium atoms, Zr_{A-C}, with one vacancy coordination, will be active towards molecule adsorption. The seven inequivalent surface oxygen atoms of the m -ZrO₂ ($\bar{1}11$) surface are two-, three-, and fourfold coordinated. With regard to oxygen reactivity, the 4-fc oxygen atom, O_e, is expected to be almost inert due to a lack of vacancy coordination, as well as the 3-fc atom, O_f, which is below the surface plane and molecule accessibility is rather limited.

Bearing in mind the previous description of zirconium and oxygen atom reactivity, the adsorption of acetic acid over the m -ZrO₂ ($\bar{1}11$) surface was investigated. For all intermediate and transition-state structures, the relative energy with respect to reactants (m -ZrO₂($\bar{1}11$) surface and two gas phase molecules of acetic acid) was evaluated at the PW91 (ΔE_{PW91}) and at the PW91-D3 ($\Delta E_{\text{PW91-D3}}$) levels, and are available in the Supporting Information. Unless stated otherwise, PW91-D3 energies are discussed below. The most stable acetic acid adsorption complexes on the m -ZrO₂ ($\bar{1}11$) surface were found when the organic molecule interacted, through the carbonyl oxygen atom, with one of the 6-fc surface zirconium atoms, Zr_A, Zr_B, or Zr_C. More than ten structures were investigated by varying the lo-

cation, orientation, and coordination of the molecule over the surface, for which interaction energies ($\Delta E_{\text{PW91-D3}}$) between -67 and -172 kJ mol⁻¹ were obtained. The reactivity of 2-fc (O_c) and 3-fc (O_a, O_b, O_d, and O_g) surface oxygen atoms towards acidic hydrogen abstraction was also investigated. It was found that H removal was a barrierless process when the reaction took place at the 2-fc coordinated oxygen atoms, O_c, whereas a barrier of 8 kJ mol⁻¹ was found in the proximity of 3-fc oxygen atoms, O_a and O_g. It is

also important to note that the intermediate adsorption species formed, after acid deprotonation, in proximity to the 2-fc oxygen atoms are about 30 kJ mol⁻¹ more stable than those formed near the 3-f coordinated O atoms.

β -Keto acid route

The reaction mechanism discussed first involves the formation of a β -keto acid intermediate, in line with the proposal by Neunhoeffer and Paschke,^[10] and is referred to herein as the β -keto acid route (Scheme 2). In Figure 5, the reaction pathway A \rightarrow B \rightarrow C \rightarrow D \rightarrow E \rightarrow F \rightarrow G \rightarrow H \rightarrow I shows schematically ketonic decarboxylation taking place along the β -keto acid route over the m -ZrO₂ ($\bar{1}11$) surface slab model. Intermediate and transition-state structures along the reaction pathway for acetic acid decarboxylation over the m -ZrO₂ ($\bar{1}11$) surface are shown in Figure 6. Selected geometrical parameters are given in Figure 7. A list of the intermediate and transition-state structures involved in each step of the reaction pathway can be found in the Supporting Information. The β -keto acid route starts with the formation of the most stable acetic acid adsorption complex (species 1 in Figures 6 and 7) with release of 172 kJ mol⁻¹. This intermediate 1 can be further stabilized by interaction of the deprotonated oxygen atom with a second zirconium atom to form a double-coordinated acetate intermediate 2. In the acetate intermediate 2, the Zr–O distances are about 2.25 Å and the C–O distances are within 1.27–1.29 Å.

Simple inspection of the geometry of intermediate 2 shown in Figure 6 immediately reveals an acetate with a negative charge. For the most relevant intermediate species, Bader's analysis of charge density is available in the Supporting Information and it has been used as a guide for naming the reaction intermediates. From acetate 2, abstraction of one out of the three α -hydrogen atoms, H_e, by the 2-fc surface oxygen atom leads to the formation of acetic acid dianion intermediate 4 via TS 3 (step B in Figure 5). This is an endothermic step, $\Delta E_{\text{rxn}} = 39$ kJ mol⁻¹, with an activation barrier of 75 kJ mol⁻¹. Formation of the dianion for adsorbed acetic acid has been recently investigated over the m -ZrO₂ ($\bar{1}11$) surface at the periodic DFT level where similar reaction energies and activation bar-

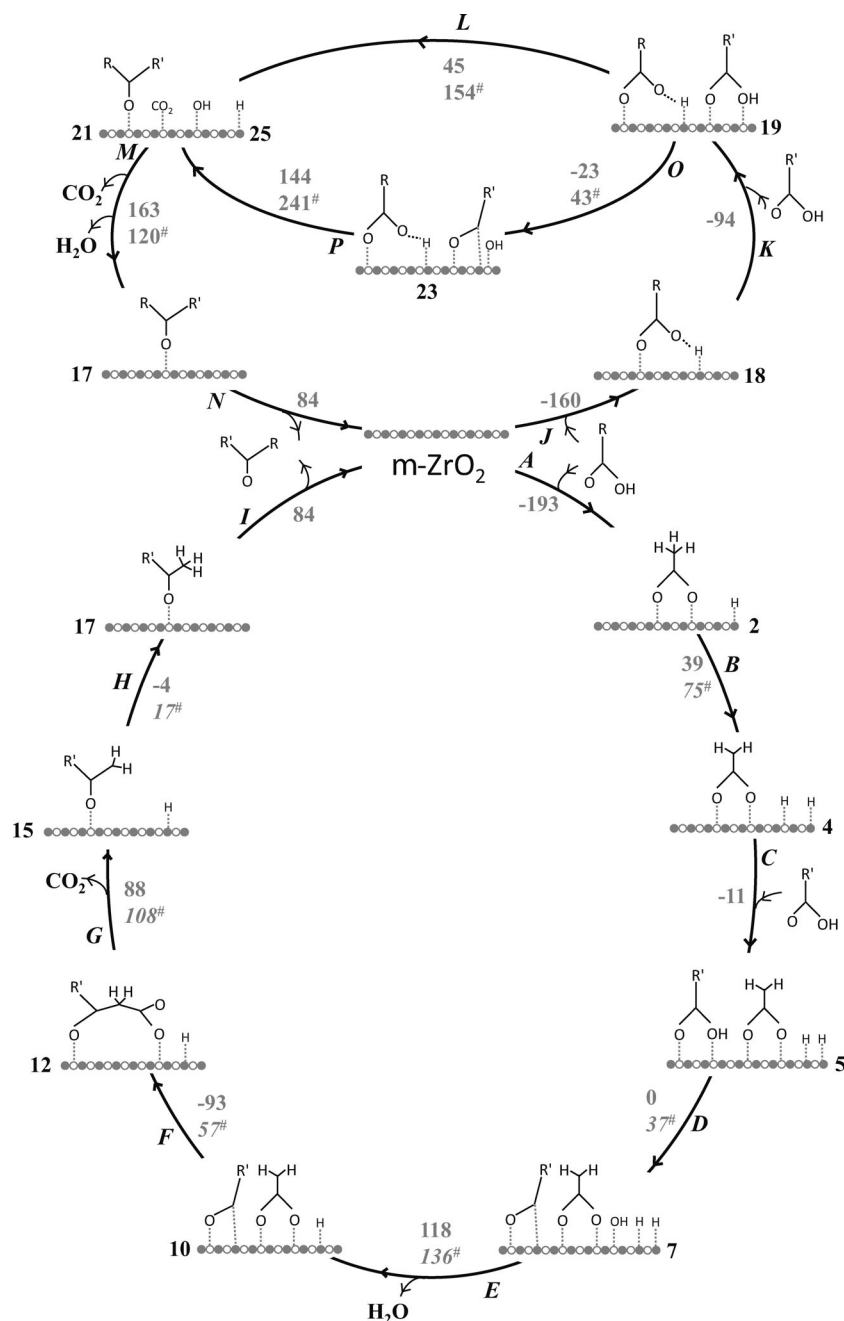


Figure 5. Reaction pathways for ketonic decarboxylation of acetic acid ($R=R'=CH_3$) over $m\text{-ZrO}_2$ following the β -keto acid (bottom) and concerted (top) routes. PW91-D3 reaction and activation (in italic and with superscript #) energies of each step are shown. Zr and O atoms of the ZrO_2 surface are represented by empty (\circ) or filled (\bullet) dots, respectively. For the sake of clarity, double bonds and charges are not displayed.

riers have been found.^[40] The reaction pathway continues (step C in Figure 5) with adsorption of a second molecule of acetic acid (structure 5) in the proximity of the previously formed dianion. The second molecule of acetic acid can be easily dehydroxylated ($E_a=37\text{ kJ mol}^{-1}$), leading to the formation of an adsorbed acylium intermediate 7 via TS 6 (step D in Figure 5), in which the C–OH bond is already partially broken with a length of 1.448 Å. At this point, a hydrogen and hydroxyl group have already been removed from the acetic acid mol-

ecules and can be combined to produce a molecule of water (step E in Figure 5). From the previously adsorbed H and OH group, in the proximity of the zirconium Zr_C atom, water formation was an endothermic process ($\Delta E_{\text{rxn}}\approx 120\text{ kJ mol}^{-1}$) that needed an activation barrier of 136 kJ mol^{-1} .

Theoretical investigations into water adsorption on the $m\text{-ZrO}_2$ ($\bar{1}\bar{1}\bar{1}$) surface has been previously carried out^[39,41] and it has been found that H_2O can adsorb to the zirconia surface molecularly or dissociatively, depending on the zirconium adsorption site and water coverage. Water adsorption processes on the $m\text{-ZrO}_2$ ($\bar{1}\bar{1}\bar{1}$) surface have been reported as exothermic ones, where energy is released in the range between 80 and 125 kJ mol^{-1} at the DFT level, which is in good agreement with our reported energy barrier for water formation at the zirconium Zr_C site (PW91 values available in the Supporting Information). After water desorption, an acetic acid dianion and an acylium intermediate are closely adsorbed on the zirconia surface (structure 10). Then the terminal CH_2 carbon atom of the dianion attacks the carbon atom of the carbonyl group of the acylium intermediate (step F in Figure 5), leading to the formation of the β -keto acid intermediate (as a carboxylate, structure 12) via TS 11, where the new C–C bond is already partially formed with a bond length of 1.825 Å (see Figure 7). This is an exothermic step (-93 kJ mol^{-1}) with an activation barrier of 57 kJ mol^{-1} . From the β -keto carboxylate intermediate 12, acetone enolate and CO_2 can be formed (step G in Figure 5) by breaking of the C–C bond (originally in the dianion fragment) via TS 13 (see Figures 6 and 7). This is an endothermic process (88 kJ mol^{-1}) with an activation barrier of 108 kJ mol^{-1} . Regardless of water formation at very unfavorable locations, this is the rate-determining step of the β -keto acid route. Acetone formation by transfer of an adsorbed H atom to the acetone enolate intermediate has a barrier of only

tion barrier of 57 kJ mol^{-1} . From the β -keto carboxylate intermediate 12, acetone enolate and CO_2 can be formed (step G in Figure 5) by breaking of the C–C bond (originally in the dianion fragment) via TS 13 (see Figures 6 and 7). This is an endothermic process (88 kJ mol^{-1}) with an activation barrier of 108 kJ mol^{-1} . Regardless of water formation at very unfavorable locations, this is the rate-determining step of the β -keto acid route. Acetone formation by transfer of an adsorbed H atom to the acetone enolate intermediate has a barrier of only

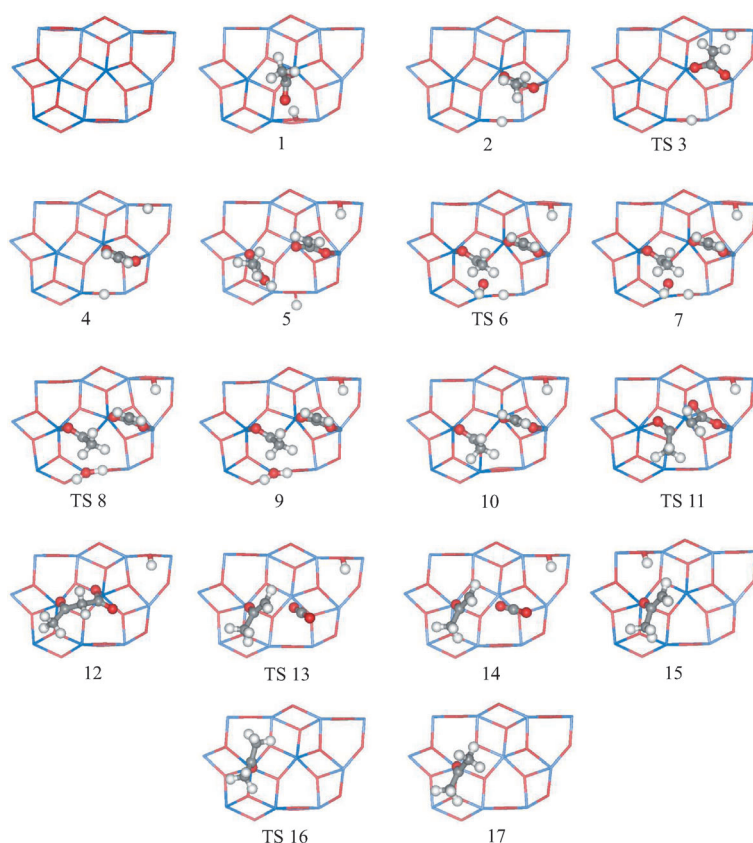


Figure 6. PW91-optimized structures involved in the β -keto acid route of acetic acid decarboxylation over m -ZrO₂. Zr and O surface atoms are depicted as light and dark gray sticks, respectively, whereas H, C, and O atoms belonging to the acetic acid molecule are depicted as white, light gray, and dark gray balls, respectively.

17 kJ mol⁻¹, in a process (step H in Figure 5) that is almost thermoneutral. The catalytic cycle is closed (step I in Figure 5) by acetone desorption, $\Delta E_{\text{rxn}} = 84$ kJ mol⁻¹.

Concerted route

A concerted reaction pathway, involving carbon–carbon bond formation and carbon dioxide formation in the same step ($J \rightarrow K \rightarrow L \rightarrow M \rightarrow N$ in Figure 5), inspired by Rand's mechanism,^[13] was also investigated for acetic acid decarboxylation over the (111) zirconia surface. Intermediate and transition-state structures along the reaction pathway were identified at the periodic DFT level and are shown in Figure 8, whereas some geometrical parameters are given in Figure 9. The concerted route also starts (step J in Figure 5) with the formation of a deprotonated acetic acid molecule on the zirconia surface (structure **18**) with release of 160 kJ mol⁻¹. Then another molecule of acetic acid needs to be weakly adsorbed in close proximity ($\Delta E_{\text{rxn}} = -94$ kJ mol⁻¹, step K in Figure 5). Thus, from the surface-adsorbed molecules (structure **19**), it is possible that the formation of acetone (structure **21**) occurs by transfer of the methyl carbanion (labeled R in the upper part of Figure 5) to the carbon atom of the carboxyl group of the other adsorbed molecule (step L in Figure 5). The formation of **TS 20** in this step shows that the new C–C bond is already partially formed and

the carbon–carbon distance is 1.555 Å, but simultaneous dehydroxylation also takes place and the C–OH distance is enlarged to 3.005 Å (see Figures 8 and 9). This is an endothermic process, +45 kJ mol⁻¹, and it is the rate-determining step of the concerted mechanism with an activation barrier of 154 kJ mol⁻¹; this is about 50 kJ mol⁻¹ higher than the rate-determining step of the β -keto acid route. At a reaction temperature of 400 °C (corresponding to a thermal energy of ≈ 8 kJ mol⁻¹), this could be considered a significant energy difference. Closing of the catalytic cycle by water, carbon dioxide, and acetone desorption would proceed as previously described for the β -keto acid route.

As an alternative reaction pathway for the concerted route, we investigated the addition of the methyl carbanion of the adsorbed acetate species to an adsorbed acylium intermediate (steps O \rightarrow P in Figure 5). This was a highly endothermic step ($\Delta E_{\text{rxn}} = 121$ kJ mol⁻¹) with a large activation energy barrier, 241 kJ mol⁻¹. Although the adsorbed acylium ion (Figure 9, structure **23**) involves an activated nucleophilic cationic carbon atom and a carbanion attack (see **TS 24** in Figures 8 and 9) could be expected to be favorable, the strong interaction between the cationic carbon atom and the oxygen surface, C...O distance of 1.301 Å, makes it a highly stabilized species and quite inert towards nucleophilic attack.

Competitive routes

The radical route was proposed for high-temperature reactions (500 °C), in which pyrolysis of carboxylic acids starts to become a competitive route.^[38] The high selectivity observed for ketonic decarboxylation over ZrO₂ indicates that cracking reactions are not very important. However, with the aim of completing the picture of the mechanism as much as possible, radical fragmentation was investigated and the question was considered as to whether surface-assisted reactions could be competitive pathways of the β -keto acid or concerted routes. For this purpose, alternative routes for the formation of adsorbed methyl species and acetone were investigated. On the one hand, homolytic breaking of the C–C bond in the adsorbed acetate intermediate **26**, generating an adsorbed methyl group (structure **27**; step Q in Figure 10), is a highly endothermic process, 278 kJ mol⁻¹, with an energy barrier greater than 275 kJ mol⁻¹. As an alternative pathway to homolytic bond cleavage in the adsorbed acetate, surface-assisted activation of the C=C double bond of the acetic acid dianion intermediate was considered (step R in Figure 10). This is also a competitive route to the formation of β -keto acid intermediate **12** from the dianion intermediate. It was found that forming a bond between the surface and the carbon atom of the CH₂ group of the dianion is an endothermic process (120 kJ mol⁻¹) with an activation energy of 272 kJ mol⁻¹ (see Figures 11 and 12). Note that these processes could occur

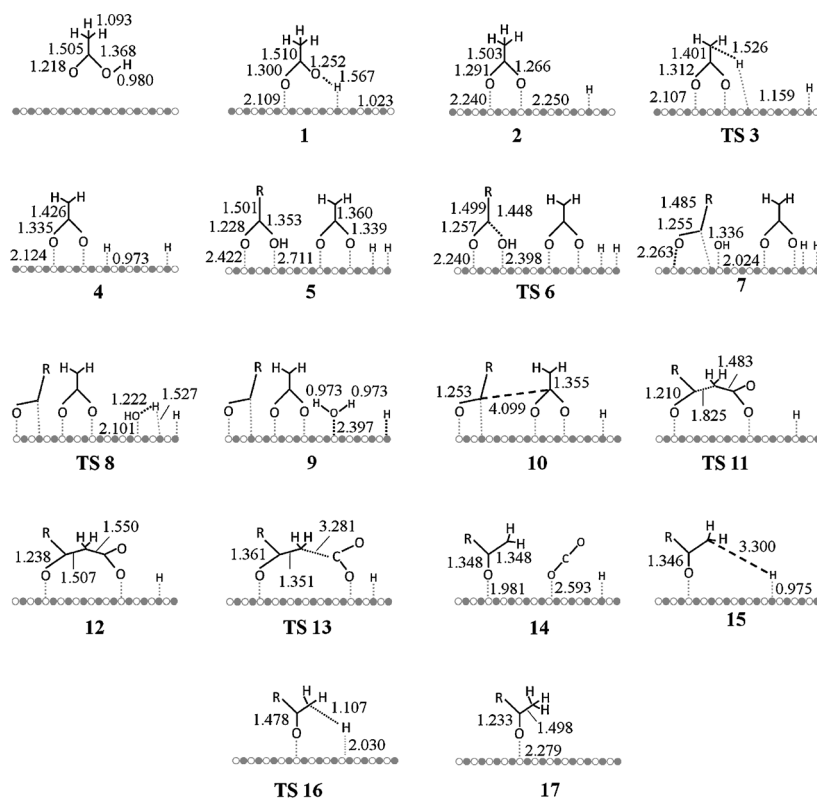


Figure 7. Geometry of the PW91-optimized structures involved in the β -keto acid route of acetic acid ($R = \text{CH}_3$) decarboxylation over $m\text{-ZrO}_2$. Distances are given in Å. Zr and O atoms of the ZrO_2 surface are represented by empty (○) or filled (●) dots, respectively. For the sake of clarity, double bonds and charges are not displayed.

during cracking of the acetic acid molecule, but are not expected to be competitive for the formation of the β -keto acid intermediate from the dianion intermediate. On the other hand, addition of the methyl group from homolytic bond cleavage to adsorbed acylium species **30** (see Figures 11 and 12), via **TS 31**, to form adsorbed acetone (structure **17**) is an exothermic process (step S in Figure 10), with the release of 119 kJ mol^{-1} and an activation barrier of 350 kJ mol^{-1} is needed.

Reaction pathways for acetic acid decarboxylation through the β -keto acid and concerted routes were also investigated at the periodic PW91 level, in addition to the PW91-D3 data discussed above. The inclusion of intermolecular dispersion interaction energies preserves the energy profile obtained at the PW91 level (see the Supporting Information). Thus, for a given elementary step, differences between calculated PW91 and PW91-D3 activation barriers are up to approximately 15 kJ mol^{-1} .

Further experimental evidence for the β -keto acid route as the ketone decarboxylation reaction mechanism

From the previously presented experimental data, we can see that $m\text{-ZrO}_2$ catalysts are promising candidates for biomass industrial transformations, but little information can be extracted concerning the reaction mechanism itself. At this point, DFT investigations favor the β -keto acid route for ketonic decarboxy-

lation of acetic acid for kinetic reasons over the concerted Rand's route involving simultaneous carbon dioxide and carbon-carbon bond formation. To test DFT predictions, ketonic decarboxylation of a mixture of two C_5 carboxylic acids, namely, valeric acid and pivalic acid, was also studied experimentally over the $m\text{-ZrO}_2$ catalyst. Valeric acid, $\text{CH}_3(\text{CH}_2)_3\text{COOH}$, has two H_α , whereas pivalic acid, $(\text{CH}_3)_3\text{C-COOH}$, has no H_α atoms (see Scheme 3). As mentioned before, when the reaction takes place with a mix of two acids, three ketones (R-CO-R , $\text{R-CO-R}'$ and $\text{R}'\text{-CO-R}'$) should be obtained in a statistical ratio of 25:50:25. Thus, from our mixture of valeric and pivalic acid, we should obtain the two symmetric ketones, $\text{CH}_3(\text{CH}_2)_3\text{CO}(\text{CH}_2)_3\text{CH}_3$ (5-nonanone), and the asymmetric one, $\text{CH}_3(\text{CH}_2)_3\text{CO-C}(\text{CH}_3)_3$ (2,2-dimethyl-3-heptanone). However,

the product distribution experimentally observed is clearly different, as shown in Scheme 3, for valeric and pivalic acid. From the results, it can be observed that 1) there is low conversion of pivalic acid (20%) compared with almost full conversion of valeric acid (99%); and 2) selectivity towards the symmetric ketone from decarboxylation of valeric acid, that is, 5-nonanone, is about 89% and towards the asymmetric ketone, 2,2-dimethyl-3-heptanone, about 4%, whereas the symmetric ketone of pivalic acid, that is, 2,2,4,4-tetramethyl-3-pentanone, is not observed at all.

In principle, 5-nonanone would be accessible by ketonic decarboxylation of valeric acid through the β -keto acid or concerted Rand's route, although based on our DFT results the β -keto acid route is the most favorable reaction pathway. Thus, the valeric acid dianion can be formed by removal of the acidic H and one of the two α -hydrogen atoms. Then, the valeric acid dianion could attack the valeric acid acylium cation to form 5-nonanone as the product or the pivalic acid acylium cation, forming 2,2-dimethyl-3-heptanone; in both cases via the corresponding β -keto acid intermediate. Formation of both adsorbed acylium ions is expected to be energetically accessible, due to the low activation energy found for acetic acid dehydroxylation. At this point, we cannot explain unambiguously the higher selectivity observed for 5-nonanone (symmetric ketone formation) with respect to 2,2-dimethyl-3-heptanone (asymmetric) when compared with the statistical ratio. First, a steric hindrance effect was considered due to the presence

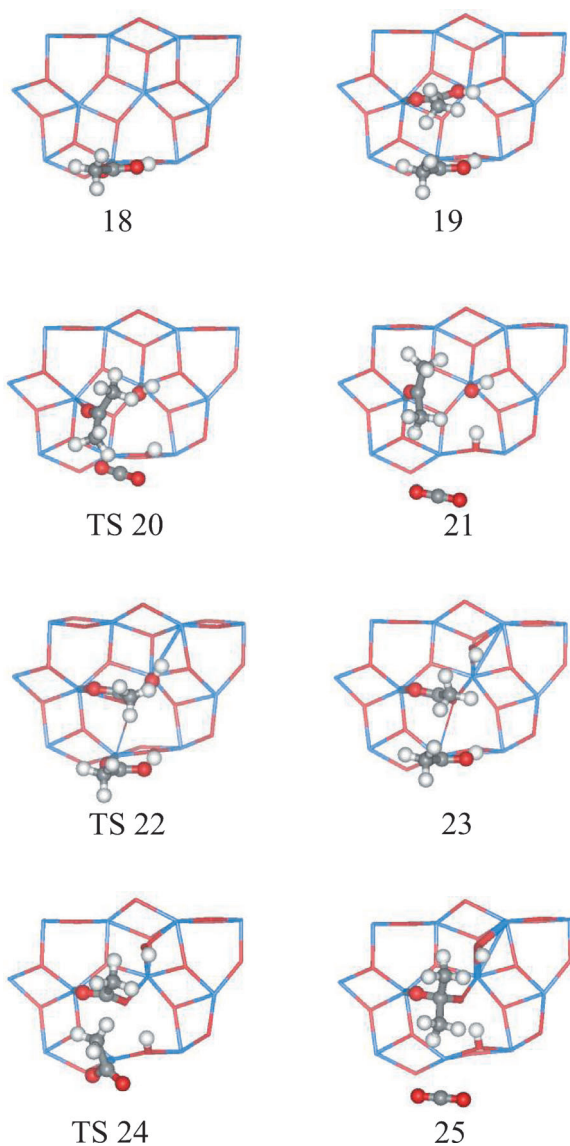


Figure 8. PW91-optimized structures involved in concerted route of acetic acid decarboxylation over $m\text{-ZrO}_2$. Zr and O surface atoms are depicted as light and dark gray sticks, respectively, whereas H, C, and O atoms belonging to the acetic acid molecule are depicted as white, light gray, and dark gray balls, respectively.

of the three methyl groups in the pivalic acid acylium cation, which makes it less likely to have both reactant fragments (valeric acid dianion and pivalic acid acylium carbocation) in close proximity. However, for a clearer understanding of this issue, a deeper study is currently under development. The ketonic decarboxylation of acetic and pivalic acid over $m\text{-ZrO}_2$ is investigated at the periodic DFT level. Thus, formation of the symmetric, $\text{CH}_3\text{-CO-CH}_3$, and asymmetric, $\text{CH}_3\text{-CO-C-(CH}_3)_3$, ketones is considered to take place by the β -keto acid and concerted route. Preliminary results show that activation barriers for ketone formation involving acetic and pivalic acid decarboxylation are larger than those obtained for decarboxylation of two molecules of acetic acid.

Formation of 2,2,4,4-tetramethyl-3-pentanone from ketonic decarboxylation of pivalic acid can only occur through the con-

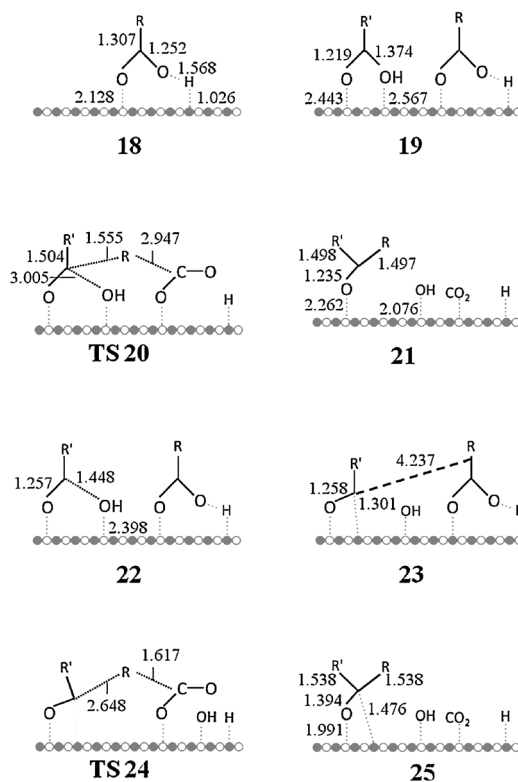


Figure 9. Geometry of the PW91-optimized structures involved in the concerted route of the acetic acid ($R=R'=\text{CH}_3$) decarboxylation over $m\text{-ZrO}_2$. Distances are given in Å. Zr and O atoms of the ZrO_2 surface are represented as empty (\circ) or filled (\bullet) dots, respectively. For the sake of clarity, double bonds and charges are not displayed.

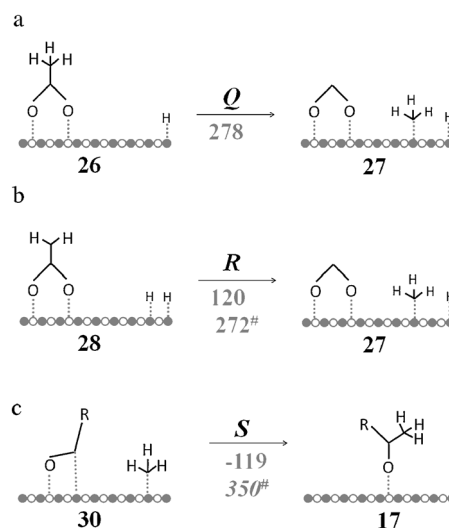


Figure 10. PW91-D3 reaction and activation (in italic and with superscript #) energies of each step are shown ($R=\text{CH}_3$). Zr and O atoms of the ZrO_2 surface are represented as empty (\circ) or filled (\bullet) dots, respectively. For the sake of clarity, double bonds and charges are not displayed.

certed Rand's route, due to the lack of α -hydrogen atoms. However, the product has not been observed and this strongly supports DFT predictions that the β -keto acid route over the $m\text{-ZrO}_2$ ($\bar{1}\bar{1}\bar{1}$) surface catalyst is kinetically favored and pre-

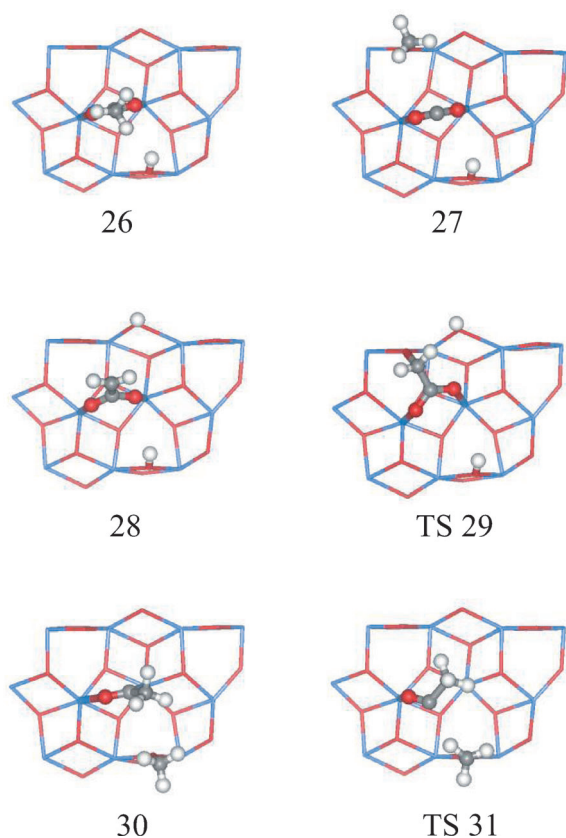
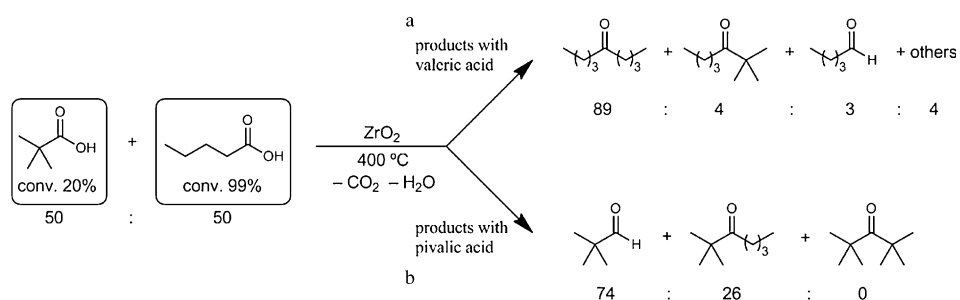


Figure 11. PW91-optimized structures involved in the competitive routes of acetic acid decarboxylation over *m*-ZrO₂. Zr and O surface atoms are depicted as light and dark gray sticks, respectively, whereas H, C, and O atoms belonging to the acetic acid molecule are depicted as white, light gray, and dark gray balls, respectively.

ferred over the concerted Rand's route. Pivalic acid decarboxylation over aerogel thoria at 490 °C has been reported by Miller et al.,^[24] leading mainly to the asymmetric *tert*-butyl isobutyl ketone with no evidence of 2,2,4,4-tetramethyl-3-pentanone formation. They explained that the reaction took place via a γ -keto acid. Alternatively, the formation of the product can be rationalized by pivalic acid isomerization with subsequent ketonic decarboxylation by the β -keto acid route, thus supporting this mechanism further. In our case, this asymmetric ketone has not been found, probably due to milder reaction conditions.



Scheme 3. Product distribution for ketone decarboxylation of a mix of valeric and pivalic acid (1:1 ratio).

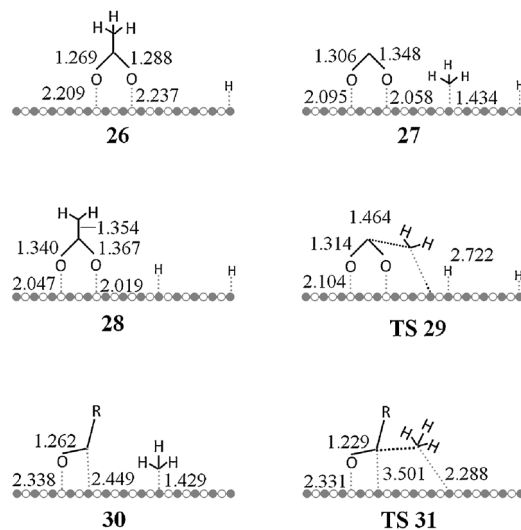


Figure 12. Geometry of the PW91-optimized structures involved in the competitive routes of acetic acid ($R = \text{CH}_3$) decarboxylation over *m*-ZrO₂. Distances are given in Å. Zr and O atoms of the ZrO₂ surface are represented by empty (○) or filled (●) dots, respectively.

Finally, it has to be stated that, from DFT, it was found that formation of the acetic acid dianion had an energy barrier of 75 kJ mol⁻¹, whereas it was only 36 kJ mol⁻¹ for the reverse reaction—protonation of the dianion. Therefore, acetic acid dianion protonation competes with β -keto acid intermediate formation that has a similar activation barrier (37 kJ mol⁻¹). Thus, although distribution of equilibrium species over the zirconia oxide surface is expected to be influenced by reaction conditions (such as gas pressure and temperature), it is concluded that the ketonic decarboxylation of monocarboxylic acids into ketones proceeds predominantly via β -keto acid intermediates.

Conclusions

Ketonic decarboxylation of carboxylic acids was carried out experimentally and studied theoretically by DFT calculations. In the experiments *m*-ZrO₂ was identified as a good catalyst, involving high activity and high selectivity when compared with other potential catalysts, such as silica, alumina, or ceria, and it was shown that it could be used for a wide range of substrates, namely, for carboxylic acids containing from two to eighteen carbon atoms.

The reaction mechanism for the ketonic decarboxylation of acetic acid over *m*-ZrO₂ was investigated by using a periodic DFT slab model. A reaction pathway with the formation of a β -keto acid intermediate was considered, as well as a concerted mechanism, involving simultaneous carbon–carbon bond formation and carbon dioxide elimination. DFT results show that the mechanism with the β -keto acid

was kinetically favored; this was further supported by an experiment employing a mixture of isomeric pentanoic acids. Therefore, the mechanism involving a β -keto acid was proposed as the predominant mechanism for the selective ketonic decarboxylation of monocarboxylic acids.

Acknowledgements

We thank MINECO (MAT2011-28009, Consolider Ingenio 2010-MULTICAT, CSD2009-00050 and CTQ2011-27550) and the Spanish National Research Council (CSIC, Es 2010RU0108) for funding. Red Española de Supercomputación (RES) and Centre de Càlcul de la Universitat de València are acknowledged for computational facilities and technical assistance. A.P. and B.O.-T. thank MINECO (Juan de la Cierva Programme) and CSIC (JAE Programme), respectively, for their fellowships.

Keywords: ab initio calculations · biomass · carboxylic acids · heterogeneous catalysis · ketones

- [1] G. W. Huber, S. Iborra, A. Corma, *Chem. Rev.* **2006**, *106*, 4044–4098.
[2] A. Corma, M. Renz, C. Schaverien, *ChemSusChem* **2008**, *1*, 739–741.
[3] D. Martin Alonso, J. Q. Bond, J. A. Dumesic, *Green Chem.* **2010**, *12*, 1493–1513.
[4] S. L. Malhotra, R. W. Wong, M. P. Breton, Xerox Corporation, US 6461417, **2002**.
[5] A. D. Tomlinson, Unilever PLC, WO 2001094522, **2001**.
[6] W. Seipel, H. Hensen, N. Boyxen, Cognis Deutschland GmbH, DE 19958521, **2001**.
[7] C. Friedel, *Justus Liebigs Ann. Chem.* **1858**, *108*, 122–125.
[8] H. Froehlich, M. Schneider, W. Himmele, M. Strohmeyer, G. Sandrock, K. Baer, EP 2758113, **1979**.
[9] H. Siegel, M. Eggersdorfer in *Ullmann's Encyclopedia of Industrial Chemistry* (Ed.: W. Gerhartz), Weinheim, VCH, **1990**, 83–95.
[10] O. Neunhoffer, P. Paschke, *Ber. Dtsch. Chem. Ges. A/B* **1939**, *72*, 919–929.
[11] Bayer & Co, DE 256622, **1911**.
[12] C. A. Smith, L. F. Theiling Jr., US 4172097, **1979**.
[13] L. Rand, W. Wagner, P. O. Warner, L. R. Kovac, *J. Org. Chem.* **1962**, *27*, 1034–1035.
[14] V. I. Yakerson, A. M. Rubinshtein, L. A. Gorskaya, GB 1208802, **1970**.
[15] M. Renz, *Eur. J. Org. Chem.* **2005**, 979–988.
[16] H. Lerner, W. Hoelderich, M. Schwarzmann, DE 3638005, **1986**.
[17] J. C. Serrano-Ruiz, D. Wang, J. A. Dumesic, *Green Chem.* **2010**, *12*, 574–577.
[18] W. A. Beavers, US 20070100166, **2007**.
[19] M. Giliński, J. Kijenski, A. Jakubowski, *Appl. Catal. A* **1995**, *128*, 209–217.
[20] A. Westfechtel, C. Breucker, B. Gutsche, L. Jeromin, H. Eierdanz, H. Baumann, K. H. Schmid, W. Nonnenkamp, DE 4121117, **1993**.
[21] R. Martinez, M. C. Huff, M. A. Barteau, *J. Catal.* **2004**, *222*, 404–409.
[22] K. Parida, H. K. Mishra, *J. Mol. Catal. A* **1999**, *139*, 73–80.
[23] A. Ignatchenko, E. Kozliak, *ACS Catal.* **2012**, *2*, 1555–1562.
[24] A. Miller, N. Cook, F. Whitmore, *J. Am. Chem. Soc.* **1950**, *72*, 2732–2735.
[25] S. Sugiyama, K. Sato, S. Yamasaki, K. Kawashiro, H. Hayashi, *Catal. Lett.* **1992**, *14*, 127–133.
[26] R. Pestman, R. M. Koster, A. v. Duijine, J. A. Z. Pieterse, V. Ponec, *J. Catal.* **1997**, *168*, 265–272.
[27] D. M. Cowan, G. H. Jeffery, A. I. Vogel, *J. Chem. Soc.* **1940**, 171–176.
[28] G. P. Hussmann, US 4754074, **1988**.
[29] E. Müller-Erlwein, B. Rosenberger, *Chem. Ing. Tech.* **1990**, *62*, 512–513.
[30] F. Wattimena, EP 85996, **1983**.
[31] S. Rajadurai, *Catal. Rev. Sci. Eng.* **1994**, *36*, 385–403.
[32] J. Cressely, D. Farkhani, A. Deluzarche, A. Kiennemann, *Mater. Chem. Phys.* **1984**, *11*, 413–431.
[33] J. C. Kuriacose, S. S. Jewur, *J. Catal.* **1977**, *50*, 330–341.
[34] V. Lorenzelli, G. Busca, N. Sheppard, *J. Catal.* **1980**, *66*, 28–35.
[35] E. Müller-Erlwein, *Chem. Ing. Tech.* **1990**, *62*, 416–417.
[36] L. J. Gooßen, P. Mamone, C. Oppel, *Adv. Synth. Catal.* **2011**, *353*, 57–63.
[37] H. Koch, E. Leibnitz, *Periodica Polytech.* **1961**, *5*, 149–185.
[38] R. A. Hites, K. Biemann, *J. Am. Chem. Soc.* **1972**, *94*, 5772–5777.
[39] A. Ignatchenko, D. G. Nealon, R. Dushane, K. Humphries, *J. Mol. Catal. A* **2006**, *256*, 57–74.
[40] A. V. Ignatchenko, *J. Phys. Chem. C* **2011**, *115*, 16012–16018.
[41] S. T. Korhonen, M. Calatayud, A. O. I. Krause, *J. Phys. Chem. C* **2008**, *112*, 6469–6476.
[42] J. C. Serrano-Ruiz, J. Luettich, A. Sepúlveda-Escribano, F. Rodríguez-Reinoso, *J. Catal.* **2006**, *241*, 45–55.
[43] F. D. Murnaghan, *Proc. Natl. Acad. Sci. USA* **1944**, *30*, 244–247.
[44] F. Birch, *Phys. Rev.* **1947**, *71*, 809–824.
[45] G. Kresse, J. Furthmüller, *Phys. Rev. B* **1996**, *54*, 11169–11186.
[46] J. P. Perdew, Y. Wang, *Phys. Rev. B* **1992**, *45*, 13244–13249.
[47] J. P. Perdew, J. A. Chevary, S. H. Vosko, K. A. Jackson, M. R. Pederson, D. J. Singh, C. Fiolhais, *Phys. Rev. B* **1992**, *46*, 6671–6687.
[48] P. E. Blöchl, *Phys. Rev. B* **1994**, *50*, 17953–17979.
[49] G. Kresse, D. Joubert, *Phys. Rev. B* **1999**, *59*, 1758–1775.
[50] A. Christensen, E. A. Carter, *Phys. Rev. B* **1998**, *58*, 8050–8064.
[51] G. Henkelman, H. Jónsson, *J. Chem. Phys.* **1999**, *111*, 7010–7022.
[52] G. Henkelman, H. Jónsson, *J. Chem. Phys.* **2000**, *113*, 9978–9985.
[53] S. Grimme, J. Antony, S. Ehrlich, H. Krieg, *J. Chem. Phys.* **2010**, *132*, 154104.
[54] <http://toc.uni-muenster.de/DFTD3/>.
[55] M. A. Barteau, *Chem. Rev.* **1996**, *96*, 1413–1430.

Received: June 18, 2012

Revised: September 14, 2012

Published online on November 30, 2012